



Contents lists available at ScienceDirect

Spectrochimica Acta Part A: Molecular and Biomolecular Spectroscopy

journal homepage: www.elsevier.com/locate/saa

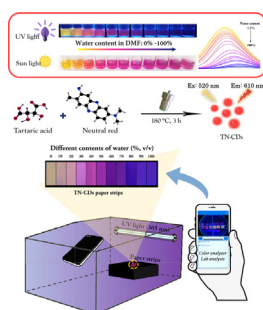
Reversible fluorescent test strip with red fluorescent carbon dots for monitoring water in organic solvents: Visual detection via a smartphone

Xiaowei Mu^a, Xiaona Song^c, Dejiang Gao^a, Pinyi Ma^{a,*}, Qiong Wu^{b,*}, Daqian Song^{a,*}^aJilin Province Research Center for Engineering and Technology of Spectral Analytical Instruments, College of Chemistry, Jilin University, Qianjin Street 2699, Changchun 130012, China^bDepartment of Gastrointestinal and Colorectal Surgery, China-Japan Union Hospital of Jilin University, Sendai Street 126, Changchun 130033, China^cChangchun Dirui Medical Company Ltd., Changchun 130012, China

HIGHLIGHTS

- A novel colorimetric and fluorescent assay for water content detection based on red-emitting carbon dots (TN-CDs) was developed.
- The assay demonstrates fast response time, good stability, and a wide detection limit.
- The assay is capable of water determination in both solution and paper test strips.
- Paper strips and smartphone were designed for quick and easy visual inspection of water content in organic solvents.

GRAPHICAL ABSTRACT



ARTICLE INFO

Article history:

Received 5 February 2022

Received in revised form 13 March 2022

Accepted 24 March 2022

Available online 26 March 2022

Keywords:

Carbon dots
Fluorescent Sensor
Water sensing
Visualization
Smartphone

ABSTRACT

Herein, a novel type of red-emitting carbon dots called TN-CDs was created via a one-step hydrothermal approach using neutral red and tartaric acid as raw materials. The fluorescence of TN-CDs was gradually quenched as the amount of water increased, and the color of the solution changed from yellow to pink mauve (or purple to pink). The reaction could be completed within only 5 s in various organic solvents such as N,N-Dimethylformamide (DMF), methanol (MeOH), acetonitrile (ACN), and ethanol (EtOH) with linear detection ranges of 1.2%–35.0%, 0.5%–20.0%, 0.25%–5.0% and 0%–16.0%, respectively. In addition, we prepared a reusable test strip and then combined it with TN-CDs to detect water content in DMF, as well as integrated it with smartphone software, a UV lamp, and a dark chamber for real-time, on-site, visual quantitative detection of the water content.

© 2022 Elsevier B.V. All rights reserved.

1. Introduction

Water (H₂O) is an inorganic substance composed of two hydrogen atoms and one oxygen atom. It is a common substance, indispensable raw material, and a pollutant for some humidity-sensitive chemicals used in organic synthesis and industrial pro-

cesses [1,2]. Chemical solvents need to have a low water content because the presence of only trace amounts of water in chemical experiments and industrial production may lead to low yields and even experimental failures [3,4]. Therefore, quantitative and qualitative analysis of moisture is required before conducting chemical reactions or industrial production processes [5–8]. Karl Fischer titration is the most widely used method for detecting water; however, this method still has many problems, such as the presence of toxic reagents, complicated operations, and the lack of portability, which have hindered its practical applications [9,10]. Therefore, there is a

* Corresponding authors.

E-mail addresses: mapinyi@jlu.edu.cn (P. Ma), qiong_wu@jlu.edu.cn (Q. Wu), songdq@jlu.edu.cn (D. Song).

need to develop a low-cost, simple, and convenient method for detecting trace amounts of water in organic media.

Thus far, a variety of fluorescent strategies, including carbon dots (CDs), quantum dots, metal nanoclusters, covalent organic frameworks (COFs), and fluorescent dyes, have been used in water content detection [11–15]. For instance, Wu and their team have developed new CDs with altered surface states using resorcinol as the only precursor for water detection in various organic solvents [16]. Wang and colleagues have constructed a crystalline COF and used it as a sensing platform that can detect water at concentrations of 7%–70% in DMF [17]. Qian and coworkers have designed glutathione-stabilized Cu nanoclusters that can sensitively respond to water based on a reverse process of aggregation-induced enhancement (AIE) mechanism [15]. Xu's group has studied a small AIE organic molecule named DMTA that can detect water in different organic solvents with broad detection ranges; and the molecule has been applied in humidity detection, water jet printing, and fingerprint information collection [18]. However, most of the described materials can only detect water in a narrow content range and rely on large instruments for fluorescence signal detection [19–21]. In contrast to the traditional fluorescence method, the smartphone-based sensing platform can detect the change of water content without the need of complicated analysis equipment [22–24]. Thus, constructing a method that is inexpensive and reversible, has fast response time, and can detect water in organic solvents in a wide content range using a smartphone-based sensing and fluorescence-based detection platform can have a significant impact on the water detection field.

Here, we report a method for preparing red-emitting TN-CDs from neutral red and tartaric acid using a one-pot method. As shown in Scheme 1, at an excitation wavelength of 520 nm, TN-CDs emit red fluorescence and exhibit interesting solvent-dependent effects. When a trace amount of water is present in the organic solvents (e.g., ACN, EtOH, MeOH, and DMF), the fluorescence of TN-CDs in the solvents gradually becomes weakened. In DMF solution, the color of the mixture can be observed with the naked eye and found to change from yellow to pink mauve as the water content increases. In addition, to develop a fast, convenient, and micro-detection method and to obtain accurate concentration results, we used paper strips and a smartphone for image acquisition, color output, and data fitting. Finally, we showed that the TN-CDs paper strips were reusable.

2. Experimental section

2.1. Chemicals and materials

Tartaric acid, *N,N*-dimethyl formamide (DMF), dimethyl sulfoxide (DMSO), acetonitrile (ACN), methanol (MeOH), ethanol (EtOH), acetone, petroleum ether (PE), dichloromethane (DCM), and ethyl acetate (EAC) were purchased from Beijing Beihua Kaiyuan Chemical Company Ltd. Neutral red and *L*-cysteine (Cys) were purchased from Shanghai Yuanye Biotechnology Company Ltd. Sucrose and *L*-Ascorbic acid were acquired from Shanghai Macklin Biochemical Company Ltd. Glutathione (GSH) was purchased from Shanghai Aladdin Chemistry Company Ltd. Deionized water obtained from a Millipore purification device (18.2 MΩ cm) was used for all the syntheses and analyses. The above organic solvents were dried using a 4 Å molecular sieve for 12 h. All the chemicals were used without further purification.

2.2. Apparatus

Fluorescence spectra were recorded on an F-2700 Spectro fluorophotometer (HITACHI Co., Ltd., Japan) with excitation slits and

emission slits of 5 nm, and a PMT Voltage of 700 V. FT-IR spectra was investigated using KBr pellets on a Nicolet Avatar360 FT-IR spectrophotometer (Thermo Fisher Scientific Inc., USA) in the range of 4000–400 cm⁻¹. Absorption spectra were recorded on a Cary 60 UV-vis spectrometer (Agilent Technologies Inc., USA). TEM images were conducted on a JEM-2100F Transmission Electron Microscope (JEOL, Japan). XPS was performed on the ESCALAB 250 spectrometer (Thermo Fisher Scientific Inc., USA). Fluorescence lifetime was obtained on the FLS920 spectrometer (Edinburgh Instrument, UK). All pH values were measured with a PHS-3C pH-Meter (INESA Scientific Inc., China). Photographing and color reading was performed by smartphone (HUAWEI P40, Huawei Technologies Co., Ltd, China).

2.3. Synthesis of TN-CDs

Briefly, 0.033 g of tartaric acid and 0.017 g of neutral red were mixed with 10 mL of ultrapure water to form a homogeneous solution. Then, the mixture was heated in a 20 mL Teflon-lined stainless steel autoclave at 180 °C for 3 h. Next, the obtained product was centrifuged at 10000 rpm for 5 min to remove the precipitates and then dialyzed against ultrapure water using 1000 Da dialysis bags. Finally, the TN-CDs solution was freeze-dried and stored until subsequent use.

2.4. Fluorescence-based detection of water in organic solvents

In a typical detection, 10 μL of 2 mg/mL TN-CDs (dissolved in DMF) was added into a DMF/water mixture to obtain samples with the final water concentrations ranging from 0 to 100% (total volume = 500 μL). After the samples were mixed thoroughly, their fluorescence emission spectra at an excitation wavelength of 520 nm were recorded. The same procedure was applied for the detection of water in MeOH, ACN, and EtOH.

2.5. Fabrication of colorimetric test strips based on TN-CDs

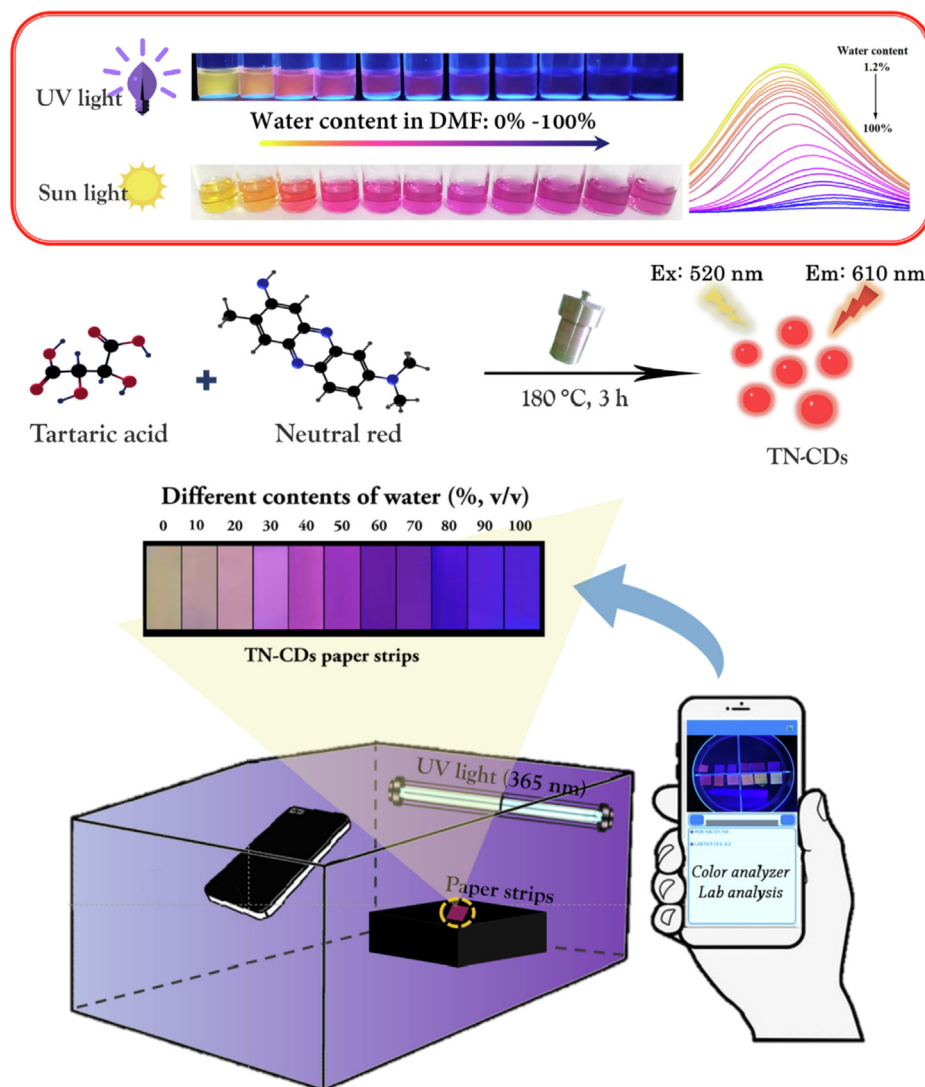
Since the prepared TN-CDs solution was colored and had good solubility in water and DMF, it was used as an ink in which filter paper strips were immersed in order to prepare a portable paper sensor. Commercial filter paper was cut into strips with an exact size of 6 cm × 1 cm to facilitate dyeing and drying. The strips were placed in a glass vial in which they were soaked in 0.02 mg/mL TN-CDs solution for 2 h. After that, the drenched filter paper was air-dried at room temperature until the remaining moisture was completely evaporated.

After drying, the prepared test strips were cut into small squares with dimensions of 1 cm × 1 cm. Subsequently, 10 μL of DMF/water mixture at different volume ratios was dropped onto the test strips using a pipette. Then, the test strips were irradiated under 365-nm UV light and their images were immediately captured using a camera on a Huawei P40 smartphone. The volume ratios of water were analyzed using a color scanning application (Color analyzer).

3. Results and discussion

3.1. Structure and morphologies of the prepared TN-CDs

The surface status of natural red and the prepared TN-CDs was characterized by Fourier transform infrared spectroscopy (FT-IR), and the result is shown in Fig. 1A. For the neutral red precursor (green line), the weak absorption bands at 3350 cm⁻¹ and 3160 cm⁻¹ could be assigned to N-H stretching vibration, while the strong absorption band at 1617 cm⁻¹ was corresponded to



Scheme 1. Illustration showing the fabrication of TN-CDs and the detection of water content in DMF with the use of paper strips and smartphone sensing platform.

C = C stretching vibration. The absorption peak at 1328 cm^{-1} was originated from C-H in-plane bending vibration. For TN-CDs (orange line), a strong signal appeared at 3414 cm^{-1} was due to O-H stretching vibration, while the other strong signal at 1735 cm^{-1} was associated with the stretching vibration of C = O in a carboxyl group. The residual absorption peaks at around 1088 and 1133 cm^{-1} were corresponded to C-O and C-C stretching vibration, respectively. In addition, X-ray photoelectron spectroscopy (XPS) analysis was conducted to assess the chemical components of TN-CDs. The complete survey XPS spectra (Fig. 1B) of TN-CDs displayed strong signals of C1s (284.8 eV) and O1s (532.0 eV) and a weak signal of N1s (401.4 eV), suggesting that the prepared TN-CDs are composed mainly of C and O elements while contain a small amount of N element. Three noticeable bands were observed in the C1s spectrum (Fig. 1C): C = C (284.8 eV), C - N (286.4 eV), and C = O (288.2 eV). The N1s peaks shown in Fig. 1D could be decomposed into 399.4 eV and 401.4 eV corresponding to C-N and N-H, respectively. The above characterization shows that the surface groups of the TN-CDs likely arise from both neutral red and tartaric acid, the indication that the TN-CDs were successfully synthesized.

The surface morphology and size of the prepared TN-CDs in water and DMF were further characterized by transmission electron microscopy (TEM). As shown in Fig. 2A, TN-CDs were well dispersed in water and had a spherical shape without apparent aggregation; their average diameter was 2.5 nm . However, when TN-CDs were dispersed in DMF, they formed aggregates (Fig. 2B). This may be due to that the surface groups of TN-CDs are more polar than DMF. Furthermore, the lattice spacing, which was calculated to be 0.22 nm and revealed by the high-resolution transmission electron microscopy (HRTEM) image (inset of Fig. 2A), was closed to the (100) plane of graphitic carbon; and this further proves that TN-CDs were successfully synthesized [25].

3.2. Optical properties of the prepared TN-CDs

The optical properties of TN-CDs were further studied by UV-vis absorption and fluorescence spectroscopy. As illustrated in Fig. 3A, the UV-vis absorption peaks of TN-CDs centered at 270 nm and 520 nm were corresponded to the $\pi-\pi^*$ transitions of C = C and the $n-\pi^*$ transitions of C = O or C - N. As can be observed in the inset of Fig. 3A, TN-CDs were dispersed in water

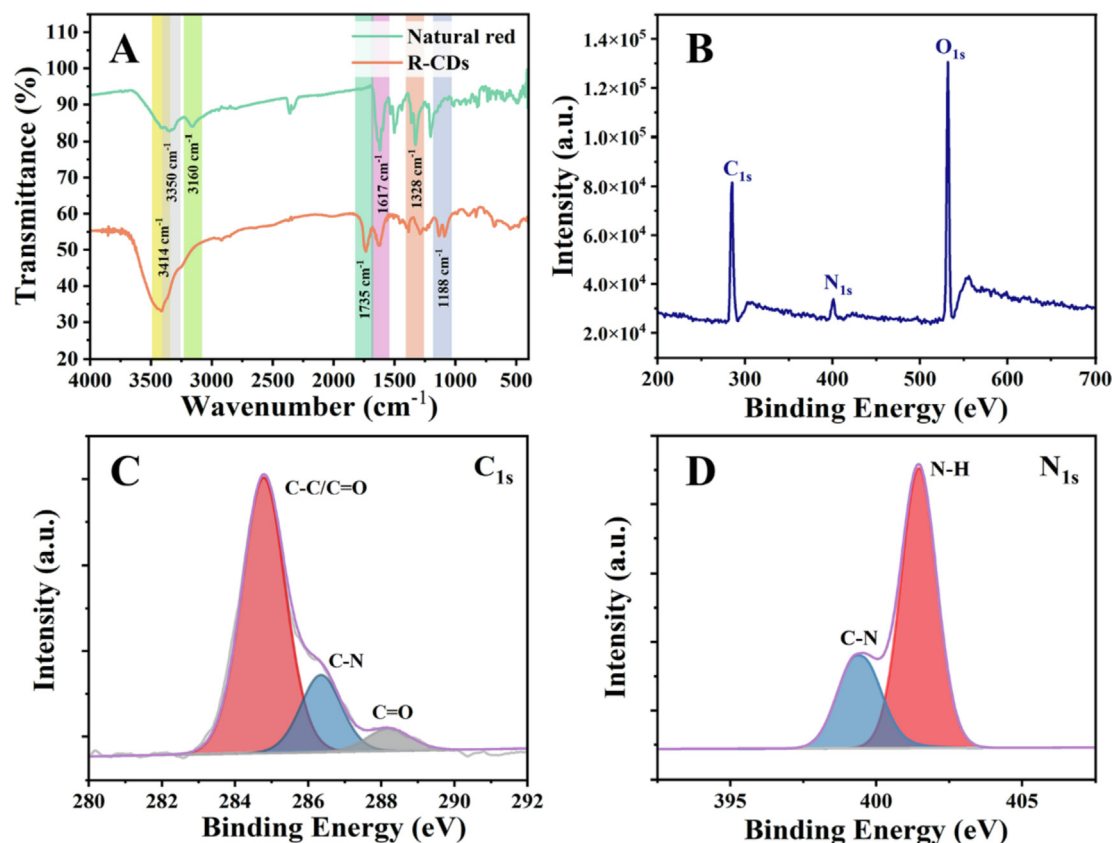


Fig. 1. (A) FT-IR spectra of natural red and TN-CDs. (B) XPS survey spectra of TN-CDs and high-resolution spectra of (C) C_{1s} and (D) N_{1s} peaks. (For interpretation of the references to color in this figure legend, the reader is referred to the web version of this article.)

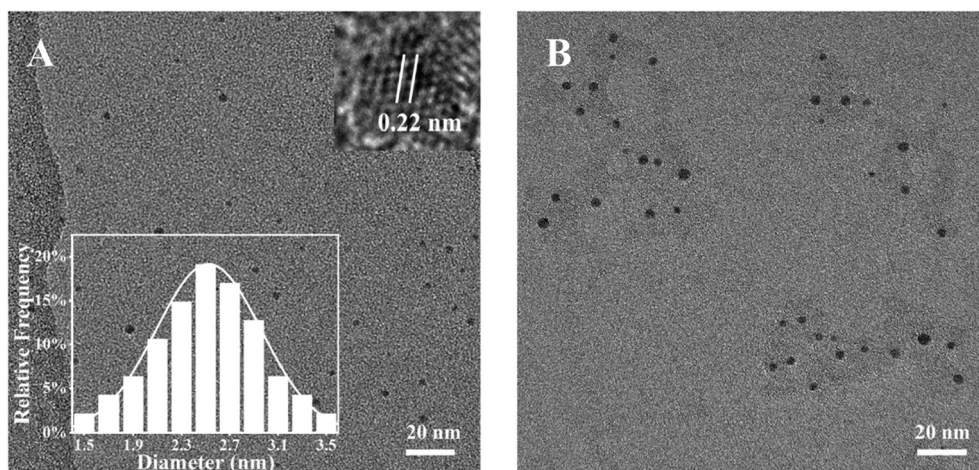


Fig. 2. (A-B) TEM images of the prepared TN-CDs in water (A) and DMF (B). The insets of (A) are the HRTEM image and size distribution.

and exhibited pink mauve color under 365-nm UV light. In addition, the fluorescence spectra of TN-CDs recorded at different excitation wavelengths are displayed in Fig. 3B, showing that the sample exhibited excitation-dependent emission behavior. As the excitation wavelength was increased from 440 nm to 580 nm at an interval of 20 nm, the emission wavelength was red-shifted from 608 nm to 616 nm. Once the excitation wavelength reached 520 nm, the intensity of the fluorescence spectra gradually decreased. Accordingly, we chose 520 nm and 610 nm as the optimum excitation and emission wavelengths, respectively. The excitation-dependent emission behavior of TN-CDs could be

ascribed to the difference in particle sizes and functional groups presented on their surface.

In addition, properties of fluorescent CDs could be affected in a complex chemical environment. As shown in Fig. S1, the fluorescence intensity of TN-CDs after 60 min of continuous irradiation (measured at three-min interval) was not changed significantly, indicating that TN-CDs have high photostability and could be used as potential fluorescent imaging agents. Furthermore, the stability of TN-CDs at different temperatures was studied. As shown in Fig. S2, when the temperature was increased from 4 °C to 45 °C, the fluorescence intensity of TN-CDs gradually increased, indicat-

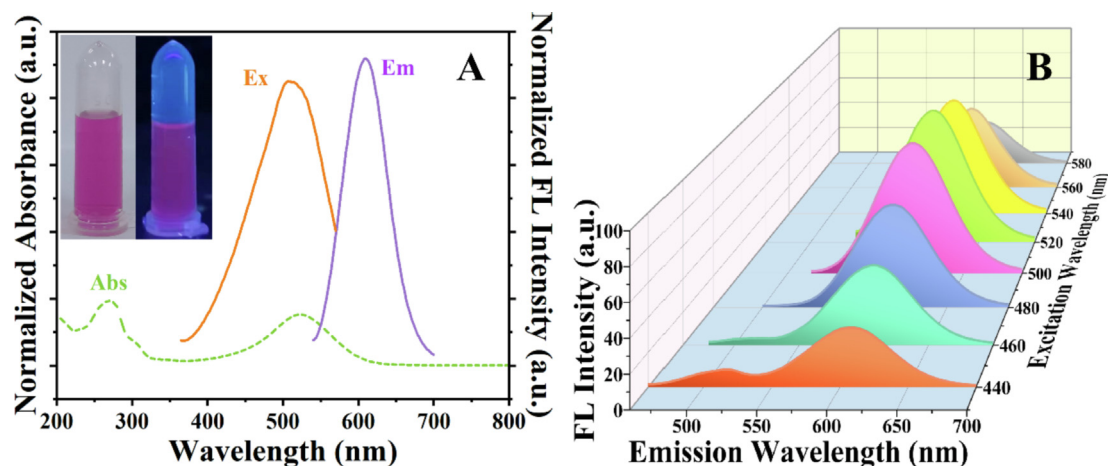


Fig. 3. (A) UV-vis absorption spectra and fluorescence excitation and emission spectra of TN-CDs. Inset: photographs of TN-CDs observed under natural light and 365-nm UV light. (B) Fluorescence emission spectra of TN-CDs recorded under different excitation wavelengths.

ing that TN-CDs are sensitive to temperature change. To diminish the effect of temperature, we conducted the experiments at a fixed temperature of 25°C.

3.3. Fluorescence-based detection of water in organic solvent using TN-CDs

We found that the fluorescence intensity of TN-CDs progressively decreased with increasing water content in DMF, MeOH, ACN, and EtOH solvents. More importantly, TN-CDs could respond to a small amount of water in DMF (a model solvent) within 5 s, which is the indication that TN-CDs have high solvatochromic sensitivity towards water. This indicates that the prepared TN-CDs may be applied to detect moisture in organic solvents in real time (Fig. S3).

DMF was used as a model solvent to illustrate their application in the monitoring of water content. Fig. 4A displays a plot of fluo-

rescence intensity ($F_0 - F$) against water content (from 1.2% to 100%) in DMF. F_0 and F are the fluorescence intensity in the absence and presence of water, respectively. Upon being excited at 520 nm, the position of the fluorescence emission peak was red-shifted from 594 nm to 620 nm while the intensity decreased gradually. Importantly, a good linear relationship ($r = 0.9965$) was observed at a range of 1.2%–35%, and the detection limit (LOD, $3\sigma/s$) was low with a value of 0.36% (Fig. 4B). As the water content in the TN-CDs/DMF system increased, the solution color changed from bright yellow to orange while then gradually changed to pink mauve. The color change could be conveniently observed under UV light with the naked eye (Fig. 4C). In addition, the prepared TN-CDs were successfully applied to detect water content at 0.5%–20%, 0.25%–5%, and 0%–16% in MeOH, ACN, and EtOH, respectively, with the corresponding LOD of 0.093%, 0.058%, and 0.042%, respectively. The corresponding linear equations and photographs are illustrated in Figs. S4, S5, and S6.

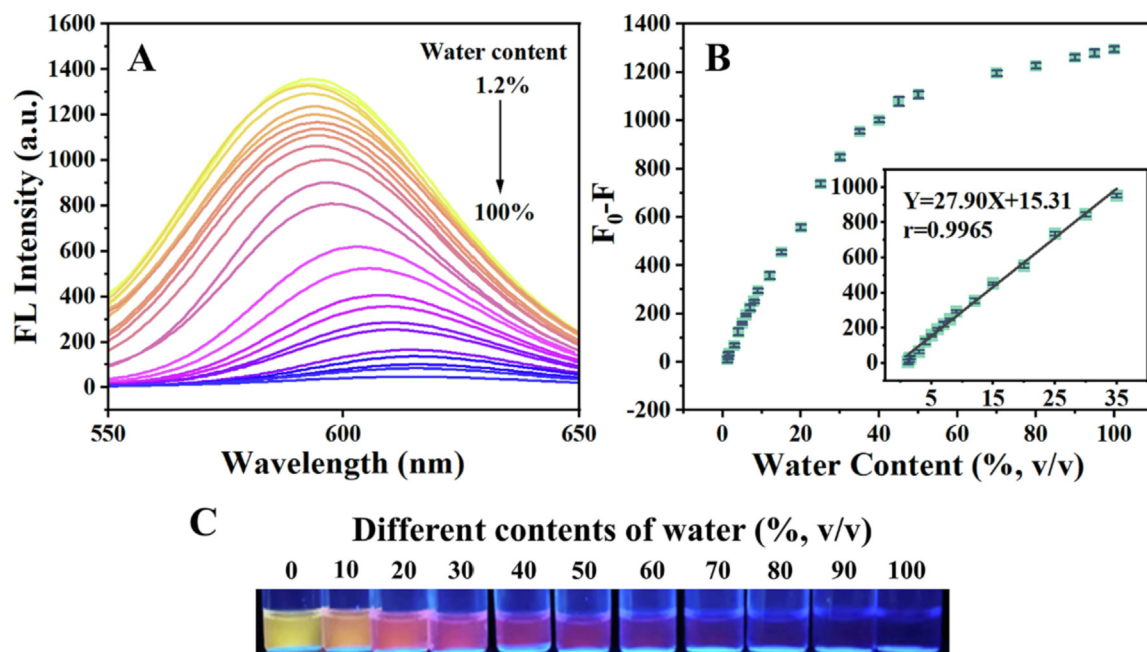


Fig. 4. (A) Emission spectra of the prepared TN-CDs in DMF containing water at an increasing level (from 1.2% to 100%). (B) Relationship between fluorescence intensity ($F_0 - F$) and water content. Inset: linear plot of $F_0 - F$ versus water content (from 1.2% to 35.0%). (C) Photographs of TN-CDs in DMF containing water at different contents (0–100%) taken under a 365 nm UV lamp.

As an example, the fluorescence intensity of the TN-CDs/DMF system remarkably decrease after H₂O was introduced, while was nearly unchanged after other common organic solvents (MeOH, acetone, DMSO, ACN, EAC, DCM, PE, and EtOH) and interference substances (AA, Cys, GSH, K⁺, Mg²⁺, and Ca²⁺) were introduced (Fig. 5A and B). The above results demonstrate that the TN-CDs/DMF system possesses good sensibility and anti-interference ability. These characteristics may essentially allow TN-CDs to have a broader potential practical application in detection of water content in DMF.

3.4. Fluorescence response mechanism of the prepared TN-CDs

Fluorescent properties of some molecules are susceptible to the polarity of the solvent; thus, the changes in solvent polarity may cause red/blue shifts in their fluorescence spectra [17,26,27]. Generally, when investigating the causes of the shift of a fluorescence spectrum, the primary factors that should be considered are solvent/solute polarity, electron donor/acceptor characteristics, solute-solute interaction caused by solvent polarity, etc. We examined the steady-state transient fluorescence spectrum of TN-CDs in solvents with different polarities (Fig. S7). The results showed that the fluorescence lifetime of TN-CDs in a solvent was not necessarily related to the solvent polarity. However, the shortest fluorescence lifetime of TN-CDs was still observed in three solvents including water, MeOH, and EtOH, which is the indication that hydrogen bonds may play an essential role in the solvation process. Under the same excitation wavelength, the shift of this fluorescence spectrum in different polar solvents can be a proof of possible hydrogen bonds between hydrophilic functional groups on the surface of TN-CDs and hydroxyl groups of the solvent. As the polarity of the protic solvent increased, the fluorescence emission peaks of TN-CDs were significantly red-shifted (Fig. S8). This could be explained by that as the water content increases, the hydrogen bonds between TN-CDs and organic solvents gradually become more controllable by the hydrogen bonds between TN-CDs and water. Since the polarity of water is highest among all solvents, its hydrogen bond interactions with the solvent can gradually increase. This can lead to changes of electron cloud distribution, which can in turn affect the conjugation degree of $\pi-\pi^*$ or $n-\pi^*$, causing its molecular energy level to decrease [17,27]. Finally, the spectrum gradually becomes red-shifted, causing the fluorescence intensity to gradually decrease, as can be observed by the change of solution color. In addition, as the reaction temperature increased, the fluorescence intensity of TN-CDs gradually increased. Such temperature-dependent fluorescence may be due

to the destruction of hydrogen bonds between hydrophilic functional groups on the surface of TN-CDs and hydroxyl groups in water, which can cause TN-CDs to have a tendency to form aggregates. The aggregation – induced enhanced emission effect can then lead to the increase of fluorescence of TN-CDs. Finally, as can be observed in the TEM image of TN-CDs in DMF, the distance between TN-CDs particles in low-polarity solvents was shorter compared with those in high-polarity solvents. Additionally, the number of aggregated particles increased significantly, causing the change of color of the solvent.

3.5. Visual inspection of water content in DMF in paper strips and solution using a smartphone application

These promising results have led us to consider using the prepared TN-CDs to coat a solid support such as paper strips. Recently, the development of sensitive and field-detection paper strips has received widespread attention [28,29]. Therefore, we developed rapid and portable TN-CDs paper strips with visual detection ability to detect water content in DMF. As shown in Fig. 6A, after dropping the samples onto the paper strips, the water content in DMF gradually increased. The color of the paper strips changed from yellow, followed by purple and finally blue-violet, showing different color shades.

Although visual inspection of paper strips is possible, it relies on the ability of human eyes to distinguish between subtle color changes, which thus may not be sensitive and accurate [30,31]. Here, a smartphone sensor device, which takes advantage of the camera's high resolution and the built-in APP, was designed to analyze color parameters during real-time detection. As shown in Scheme 1, the sensing device consists of a UV excitation light source, a sample platform, a smartphone, and a dark chamber. The color parameters were analyzed using the image processing application (color analyzer), and the regression analysis was performed using the data analysis application. The Lab color mode has more color gradients than the RGB and CMYK models, thus can recognize more colors than other mode. In the Lab color mode, *L* represents brightness, *a* represents the color range from magenta to green, and *b* represents the color range from yellow to blue. The color data are shown in Table 1 & S1. The variation of *L*, *a*, *b* and *R*, *G*, *B* values with water contents measured from the paper strip is displayed in Fig. 6B and that measured from the solution is shown in Fig. S9. As can be seen, the *L* and *b* values decreased with the increase of water content, while the *a* value remained fairly stable. In addition, the *R* and *G* values decreased with the increase of water content, while the *B* value was relatively stable. The calcula-

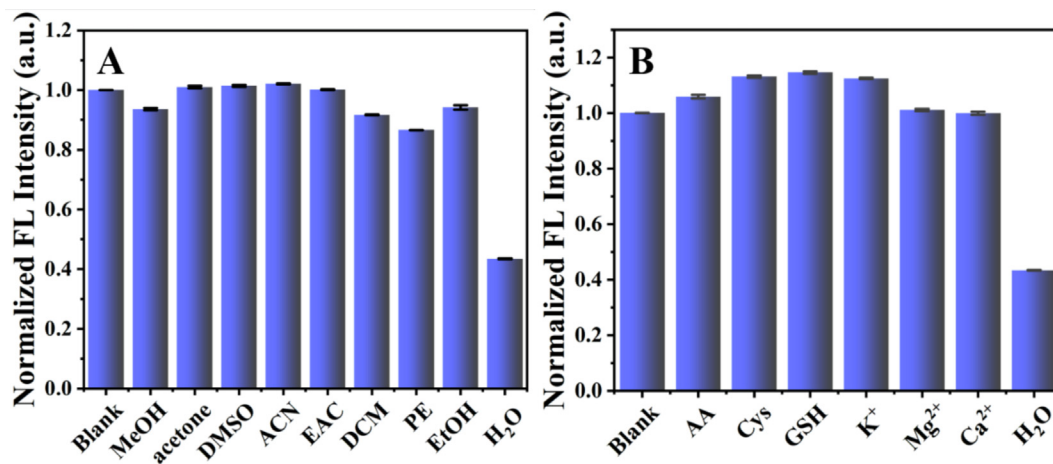


Fig. 5. Selectivity of the prepared TN-CDs measured in DMF solution (90%, v/v) toward (A) various organic solvents (10%, v/v) and (B) commonly found co-existing substances.

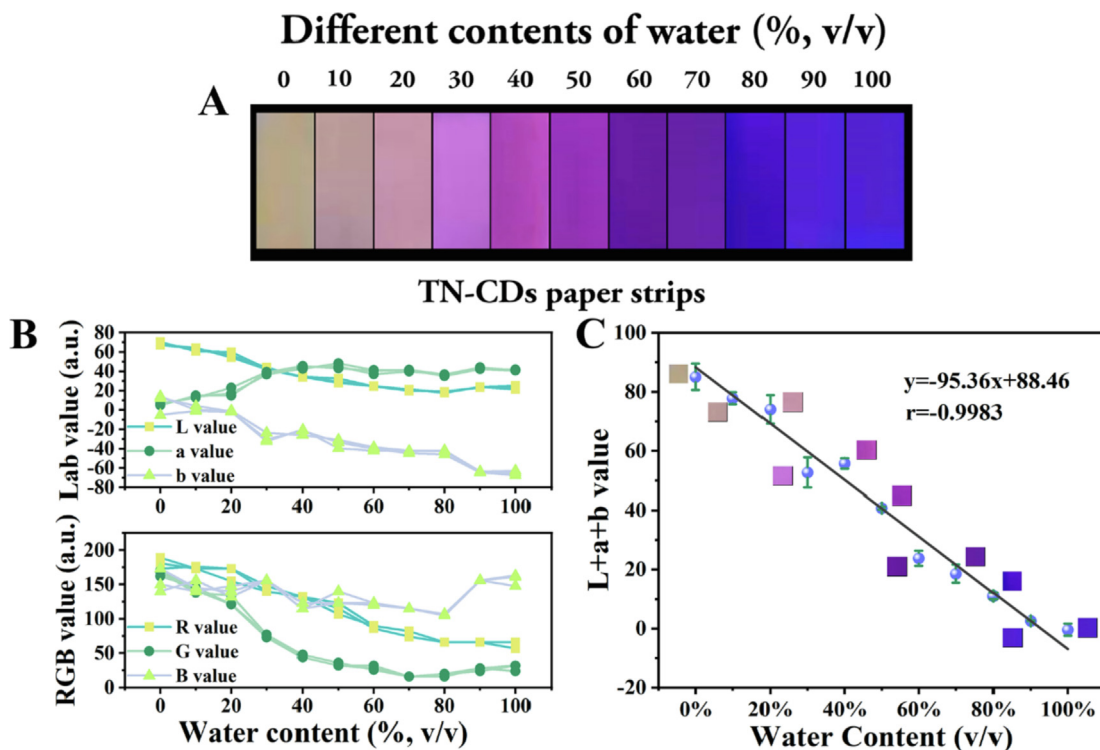













Fig. 6. (A) Photographs of TN-CDs-impregnated paper strips in DMF containing different water contents taken under a 365 nm UV lamp. (B) Change of color in Lab and RGB modes of TN-CDs paper strips. (C) Linear relationship between L + a + b value and water content in DMF.

Table 1
Visual inspection of water content in DMF through the color parameters of paper strips obtained using a smartphone application.

Color	water content (%)	R value	G value	B value	L value	a value	b value	L + a + b value
	100	57	24	148	21.4	40.8	-62.8	-0.6
	90	66	28	156	23.9	42.3	-63.6	2.6
	80	66	20	107	18.4	35.1	-41.8	11.7
	70	82	16	115	21.2	41.5	-42.3	20.4
	60	90	28	123	24.8	40.4	-38.6	26.6
	50	107	32	123	28.1	43.1	-30.9	40.3
	40	132	44	123	34.3	45.3	-25.9	53.7
	30	140	73	156	42.2	38.9	-23.5	57.6
	20	155	121	132	54.4	15	-0.7	68.7
	10	173	146	156	64.1	14.8	0	78.9
	0	181	162	140	67.9	4.9	14.2	87

tion showed a linear relationship between L + a + b and water content. Photographs of paper strips and solutions containing DMF with different water contents were taken, and the calibration equa-

tion was established (Fig. 6C & S10). For the paper strips, the L + a + b value was proportional to the water content, and the solution color gradually changed from beige to blue-violet. A linear

relationship between the $L + a + b$ value and the water content at a range of 0–100%, which could be used to calculate the water content, could be expressed as $y = -95.36x + 88.46$ ($r = -0.9983$). In the solution, the value of $L + a + b$ decreased with increasing water content (10%–60%). The relationship was linear and could be expressed as $y = -230.71x + 149.79$ ($r = -0.9989$), and the color of the paper strip gradually changed from orange to purple.

As illustrated in Table S2, we detected 5 samples spiked with water at different contents using test strips and a smartphone. The results showed that samples with higher water contents (>35%) have higher recovery rates, and the RSD values of all the five samples were less than 3.5%. Additionally, we explored the reusability of the paper strips. First, the color of the dry paper strip was pink. After a moist paper strip was soaked in DMF solvent and then heated using a hot air blower, its color was returned from yellow to pink within ten seconds. The above steps were repeated, and the color of the paper strip was not significantly changed after 3 rounds (Fig. S11). All in all, our method has reasonable practicability and fast response; its quantitative analysis can be accomplished through visual inspection using test strips and a smartphone, thus is highly suitable for on-site detection of water content in DMF.

4. Conclusion

In short, we synthesized red-emitting CDs through a simple one-step hydrothermal synthesis method using tartaric acid and natural red solution as reaction precursors. The synthesized TN-CDs could detect water content in an organic solvent through fluorescence signals and color change. TN-CDs had fast response time, good stability, and a wide detection limit. In addition, we designed a device consisting a smartphone, a UV light source, and a dark chamber for visual detection of water content in DMF. The smartphone APP was employed to analyze the color change of the paper strips irradiated with UV light and quantify the water content. The detection was linear at the water contents of 0–100%, and the correlation coefficient r was as high as 0.9983 while RSD values of the spiked samples were $\leq 3.5\%$. The developed device has not only high accuracy and fast response time, which could further expand its application in field-detection of water content in organic solvents.

The authors declare that they have no known competing financial interests or personal relationships that could have appeared to influence the work reported in this paper.

CRedit authorship contribution statement

Xiaowei Mu: Conceptualization, Data curation, Formal analysis, Investigation, Validation, Writing – original draft. **Xiaona Song:** Data curation, Investigation. **Dejiang Gao:** Writing – review & editing, Formal analysis. **Pinyi Ma:** Conceptualization, Project administration, Data curation, Writing – review & editing. **Qiong Wu:** Investigation, Resources, Writing – review & editing. **Daqian Song:** Project administration, Funding acquisition, Resources, Supervision.

Declaration of Competing Interest

The authors declare that they have no known competing financial interests or personal relationships that could have appeared to influence the work reported in this paper.

Acknowledgement

This work was supported by the National Natural Science Foundation of China (Grant Nos. 22004046 and 22074052).

Appendix A. Supplementary material

Supplementary data to this article can be found online at <https://doi.org/10.1016/j.saa.2022.121195>.

References

- [1] J. Bitten, New method for determining free-water content in fuel, *Anal. Chem.* 40 (1968) 960–962.
- [2] S.-I. Ohira, Y. Miki, T. Matsuzaki, N. Nakamura, Y.-K. Sato, Y. Hirose, K. Toda, A fiber optic sensor with a metal organic framework as a sensing material for trace levels of water in industrial gases, *Anal. Chim. Acta* 886 (2015) 188–193.
- [3] Q. Wang, X. Li, L. Wang, Y. Cheng, G. Xie, Effect of Water Content on the Kinetics of p-Xylene Liquid-Phase Catalytic Oxidation to Terephthalic Acid, *Ind. Eng. Chem. Res.* 44 (2005) 4518–4522.
- [4] M.G. Gichinga, S. Striegler, Effect of Water on the Catalytic Oxidation of Catechols, *J. Am. Chem. Soc.* 130 (2008) 5150–5156.
- [5] H. An, T. Habib, S. Shah, H. Gao, A. Patel, I. Echols, X. Zhao, M. Radovic, M.J. Green, J.L. Lutkenhaus, Water Sorption in MXene/Polyelectrolyte Multilayers for Ultrafast Humidity Sensing, *ACS Appl. Nano Mater.* 2 (2019) 948–955.
- [6] S. Tsumura, T. Enoki, Y. Ooyama, A colorimetric and fluorescent sensor for water in acetonitrile based on intramolecular charge transfer: D-(π -A)²-type pyridine–boron trifluoride complex, *Chem. Commun.* 54 (2018) 10144–10147.
- [7] Y. Dong, J. Cai, Q. Fang, X. You, Y. Chi, Dual-Emission of Lanthanide Metal-Organic Frameworks Encapsulating Carbon-Based Dots for Ratiometric Detection of Water in Organic Solvents, *Anal. Chem.* 88 (2016) 1748–1752.
- [8] S.A. Yoon, J.H. Oh, S.K. Kim, M.H. Lee, Water-sensitive ratiometric fluorescent probes and application to test strip for rapid and reversible detection of water, *Dyes Pigm.* 165 (2019) 421–428.
- [9] F.K. Neues, Verfahren zur maanalytischen Bestimmung des Wassergehaltes von Flüssigkeiten und festen Krpern, *Angew. Chem.* 48 (1935) 394–396.
- [10] Y.Y. Liang, Automation of Karl Fischer water titration by flow injection sampling, *Anal. Chem.* 62 (1990) 2504–2506.
- [11] A. Douvali, A.C. Tsipis, S.V. Eliseeva, S. Petoud, G.S. Papaefstathiou, C.D. Malliakas, I. Papadas, G.S. Armatas, I. Margiolaki, M.G. Kanatzidis, T. Lazarides, M.J. Manos, Turn-On Luminescence Sensing and Real-Time Detection of Traces of Water in Organic Solvents by a Flexible Metal–Organic Framework, *Angew. Chem. Int. Ed.*, 54 (2015) 1651–1656.
- [12] Y.N. Wijaya, J. Kim, S.H. Hur, S.H. Park, M.H. Kim, Metal nanocrystal-based sensing platform for the quantification of water in water-ethanol mixtures, *Sensor. Actuator. B Chem.* 263 (2018) 59–68.
- [13] H. Li, W. Han, R. Lv, A. Zhai, X.-L. Li, W. Gu, X. Liu, Dual-Function Mixed-Lanthanide Metal-Organic Framework for Ratiometric Water Detection in Bioethanol and Temperature Sensing, *Anal. Chem.* 91 (2019) 2148–2154.
- [14] S. Pawar, U.K. Togiti, A. Bhattacharya, A. Nag, Functionalized Chitosan-Carbon Dots: A Fluorescent Probe for Detecting Trace Amount of Water in Organic Solvents, *ACS Omega* 4 (2019) 11301–11311.
- [15] Y. Huang, W. Liu, H. Feng, Y. Ye, C. Tang, H. Ao, M. Zhao, G. Chen, J. Chen, Z. Qian, Luminescent Nanoswitch Based on Organic-Phase Copper Nanoclusters for Sensitive Detection of Trace Amount of Water in Organic Solvents, *Anal. Chem.* 88 (2016) 7429–7434.
- [16] C. Ye, Y. Qin, P. Huang, A. Chen, F.-Y. Wu, Facile synthesis of carbon nanodots with surface state-modulated fluorescence for highly sensitive and real-time detection of water in organic solvents, *Anal. Chim. Acta* 1034 (2018) 144–152.
- [17] Y. Chen, C. Zhang, J. Xie, H. Li, W. Dai, Q. Deng, S. Wang, Covalent organic frameworks as a sensing platform for water in organic solvent over a broad concentration range, *Anal. Chim. Acta* 1109 (2020) 114–121.
- [18] D. Wang, H. Zhao, H. Li, S. Sun, Y. Xu, A fluorescent “glue” of water triggered by hydrogen-bonding cross-linking, *J. Mater. Chem. C* 4 (2016) 11050–11054.
- [19] T.-I. Kim, Y. Kim, A Water Indicator Strip: Instantaneous Fluorogenic Detection of Water in Organic Solvents, Drugs, and Foodstuffs, *Anal. Chem.* 89 (2017) 3768–3772.
- [20] J. Wang, X. Zhang, H.-B. Liu, Highly sensitive pyrene–dansyl conjugate-based fluorescent sensor for discriminative detection of water in organic solvents, *Dyes Pigm.* 182 (2020) 108685.
- [21] Y. Zhou, D. Zhang, W. Xing, J. Cuan, Y. Hu, Y. Cao, N. Gan, Ratiometric and Turn-On Luminescence Detection of Water in Organic Solvents Using a Responsive Europium–Organic Framework, *Anal. Chem.* 91 (2019) 4845–4851.
- [22] N. Kong, H. Yuan, H. Zhou, Y. Zhao, S. Zhang, Colorimetric detection of water content in organic solvents via a smartphone with fluorescent Ag nanoclusters, *Anal. Methods* 13 (2021) 2722–2727.
- [23] S. Chu, H. Wang, X. Ling, S. Yu, L. Yang, C. Jiang, A Portable Smartphone Platform Using a Ratiometric Fluorescent Paper Strip for Visual Quantitative Sensing, *ACS Appl. Mater. Interfaces* 12 (2020) 12962–12971.
- [24] W.-I. Lee, S. Shrivastava, L.-T. Duy, B. Yeong Kim, Y.-M. Son, N.-E. Lee, A smartphone imaging-based label-free and dual-wavelength fluorescent

- biosensor with high sensitivity and accuracy, *Biosens. Bioelectron.* 94 (2017) 643–650.
- [25] L. Li, L. Shi, J. Jia, O. Eltayeb, W. Lu, Y. Tang, C. Dong, S. Shuang, Red fluorescent carbon dots for tetracycline antibiotics and pH discrimination from aggregation-induced emission mechanism, *Sensor. Actuat. B Chem.* 332 (2021) 129513.
- [26] J. Li, P. Du, J. Chen, S. Huo, Z. Han, Y. Deng, Y. Chen, X. Lu, Dual-Channel Luminescent Signal Readout Strategy for Classifying Aprotic/Protic Polar Organic Medium and Naked-Eye Monitoring of Water in Organic Solvents, *Anal. Chem.* 92 (2020) 8974–8982.
- [27] J. Yang, Z. Li, Q. Jia, Design of dual-emission fluorescence sensor based on Cu nanoclusters with solvent-dependent effects: Visual detection of water via a smartphone, *Sensor. Actuator. B Chem.* 297 (2019) 126807.
- [28] P. Kumar, R. Sakla, A. Ghosh, D.A. Jose, Reversible Colorimetric Sensor for Moisture Detection in Organic Solvents and Application in Inkless Writing, *ACS Appl. Mater. Interfaces* 9 (2017) 25600–25605.
- [29] H. Wang, L. Da, L. Yang, S. Chu, F. Yang, S. Yu, C. Jiang, Colorimetric fluorescent paper strip with smartphone platform for quantitative detection of cadmium ions in real samples, *J. Hazard. Mater.* 392 (2020) 122506.
- [30] W. Li, X. Zhang, X. Hu, Y. Shi, Z. Li, X. Huang, W. Zhang, D. Zhang, X. Zou, J. Shi, A smartphone-integrated ratiometric fluorescence sensor for visual detection of cadmium ions, *J. Hazard. Mater.* 408 (2021) 124872.
- [31] W. Taron, K. Phooplub, S. Sanchimplee, K. Piyanamvanich, W. Jannongkan, A. Techasen, J. Phetcharaburanin, P. Klanrit, N. Namwat, N. Khuntikeo, T. Boonmars, P. Sithithaworn, S. Ouiganon, P. Kanatharana, P. Thavarungkul, C. Buranachai, W. Loilome, W. Ngeontae, Smartphone-based fluorescent ELISA with simple fluorescent enhancement strategy for *Opisthorchis viverrini* (Ov) antigen detection in urine samples, *Sensor. Actuator. B Chem.*, 348 (2021) 130705.